



ELSEVIER

Available online at www.sciencedirect.com

SCIENCE @ DIRECT®

Physics Letters A 323 (2004) 427–433

PHYSICS LETTERS A

www.elsevier.com/locate/pla

The penetrable-sphere fluid in the high-temperature, high-density limit

Luis Acedo, Andrés Santos*

Departamento de Física, Universidad de Extremadura, 06071 Badajoz, Spain

Received 1 October 2003; accepted 13 February 2004

Communicated by A.R. Bishop

Abstract

We consider a fluid of d -dimensional spherical particles interacting via a pair potential $\phi(r)$ which takes a finite value ϵ if the two spheres are overlapped ($r < \sigma$) and 0 otherwise. This penetrable-sphere model has been proposed to describe the effective interaction of micelles in a solvent. We derive the structural and thermodynamic functions in the limit where the reduced temperature $k_B T/\epsilon$ and density $\rho\sigma^d$ tend to infinity, their ratio being kept finite. The fluid exhibits a spinodal instability at a certain maximum scaled density where the correlation length diverges and a crystalline phase appears, even in the one-dimensional model. By using a simple free-volume theory for the solid phase of the model, the fluid–solid phase transition is located.

© 2004 Elsevier B.V. All rights reserved.

PACS: 61.20.-p; 64.70.Dv; 64.60.-i; 61.25.Hq

Keywords: Penetrable-sphere model; Soft interactions; Spinodal instability; Fluid–solid phase transition

Most of the theoretical studies and numerical applications of the theory of liquids in equilibrium is devoted to particles which interact according to unbounded spherically symmetric pair potentials [1,2]. Atomic and molecular fluids have been usually modeled in this way and a vast effort was done during the second half of the past century in order to understand systems such as hard spheres, the square-well model, or the Lennard–Jones liquid. The development of the integral equations of the theory of liquids, the

Percus–Yevick (PY) approximation being among the most widely used in this context, and their solution for some simple models [1–3] were landmarks in the history of the theory of liquids.

In the last decade, the properties of fluids of particles interacting via *bounded* pair potentials have been the subject of an increasing interest, the Gaussian core model [4–6] and the penetrable-sphere model [5–13] being among the most popular ones. The motivation for the study of fluids based upon this new class of interactions is two-fold. First, from a fundamental point of view, they are useful to unveil the weaknesses of standard integral equation theories and other approximations whose validity has only been assessed from applications to unbounded potentials. More consis-

* Corresponding author.

E-mail addresses: acedo@unex.es (L. Acedo), andres@unex.es (A. Santos).

URL: <http://www.unex.es/fisteor/andres/>.

tent closure approximations arise from these studies [10,11]. From a more practical point of view, these models have also been proposed in order to understand the peculiar behavior of some colloidal systems, such as micelles in a solvent or star copolymer suspensions. The particles in these colloids are constituted by a small core surrounded by several attached polymeric arms. As a consequence of their structure, two or more of these particles allow a considerable degree of overlapping with a small energy cost [6]. An ultrasoft logarithmically divergent potential for short distances has also been proposed to describe the effective interaction between star polymers in good solvents [14]. These are a few particular cases of systems defining what is commonly known as “soft matter”, which has become an active field of research with many potential physical, chemical and engineering applications.

The penetrable-sphere (PS) interaction potential is defined as

$$\phi(r) = \begin{cases} \epsilon, & r < \sigma, \\ 0, & r > \sigma. \end{cases} \quad (1)$$

This model was suggested by Marquest and Witten [15] in the late eighties as a simple theoretical approach to the explanation of the experimentally observed crystallization of copolymer mesophases, where a simple cubic solid phase coexists with the disordered suspension. By arguments based on the internal energy alone, these authors claimed that, under the assumption of single-site occupancy, the stability of the simple cubic crystal was assured in a given domain of the phase diagram. On the other hand, density-functional theory [8,9] predicts a freezing transition to fcc solid phases with multiply occupied lattice sites. The existence of clusters of overlapped particles (or “clumps”) in the PS crystal and glass was already pointed out by Klein et al. [7], who also performed Monte Carlo simulations on the system. In the fluid phase, the standard integral equation theories (e.g., PY and HNC) are not very reliable in describing the structure of the PS fluid, especially inside the core [8]. Other more sophisticated closures [10], as well as Rosenfeld’s fundamental-measure theory [11], are able to predict the correlations functions with high precision but, on the other hand, the signature for a spatially ordered phase [a divergent structure factor $S(k)$ for a finite wavenumber k] is not found with these methods. Recently, a mixture of colloids and

non-interacting polymer coils has been studied [12], where the colloid–colloid interaction is assumed to be that of hard spheres and the colloid–polymer interaction is described by the PS model. The inhomogeneous structure of penetrable spheres in a spherical pore has also been investigated [13].

In order to shed further light on the properties of the PS system, in this Letter we focus on the high-temperature, high-density region of the phase diagram. As we will see later, this asymptotic region is mathematically equivalent to taking $\epsilon \rightarrow 0$ and $\sigma \rightarrow \infty$ in a scaled way, so that we recover rigorous results first derived by Gates [16] and by Grewe and Klein [17] in the more general framework of a class of Kac potentials. At the level of the thermodynamic properties, only zeroth-order results were given in Ref. [17], but here we provide the explicit first-order corrections. Moreover, we combine the exact free energy of the PS fluid with a free-volume estimate for the free energy of the PS crystal to obtain the freezing and melting points.

We start by observing that the Mayer function of the PS interaction is simply

$$f_{\text{PS}}(r) = \exp[-\phi(r)/k_B T] - 1 = x f_{\text{HS}}(r), \quad (2)$$

where $x \equiv 1 - e^{-\epsilon/k_B T}$ is a parameter measuring the temperature of the system, $f_{\text{HS}}(r) = -\Theta(\sigma - r)$ is the Mayer function of a hard-sphere (HS) system (Θ being the Heaviside step function), k_B is the Boltzmann constant and T is the absolute temperature. Obviously, the PS model includes the HS fluid ($T \rightarrow 0$ or $x \rightarrow 1$) and the point-particle fluid ($T \rightarrow \infty$ or $x \rightarrow 0$) as special limits. The latter limit is assumed at finite number density ρ . However, a non-trivial limit is obtained if $x \rightarrow 0$ and $\rho \rightarrow \infty$ keeping the product (scaled density) $\hat{\rho} = \rho x$ finite. Although for high temperatures one has $x \approx \epsilon/k_B T$, it is more convenient to work with x rather than with $k_B T/\epsilon$ as the control parameter.

Let us consider now the exact virial expansion of the cavity function $y(r) \equiv g(r) \exp[\phi(r)/k_B T]$, where $g(r)$ is the radial distribution function [1]. In the diagrammatic representation of the virial expansion of $y(r)$, each bond in a given diagram represents a Mayer function $f_{\text{PS}}(r) = x f_{\text{HS}}(r)$. Therefore,

$$y(r) = 1 + \sum_{n=1}^{\infty} \rho^n x^{n+1} \sum_{m=0}^{n(n+1)/2-1} x^m y_n^{(m)}(r), \quad (3)$$

where the HS function $y_n^{(m)}(r)$ is represented by the sum of diagrams having 2 root points (white circles), n field points (black circles) and $n + 1 + m$ bonds. Setting $x = 1$ (zero-temperature limit), Eq. (3) becomes the virial series for hard spheres. On the other hand, in the high-temperature limit $x \rightarrow 0$ with $\rho \rightarrow \infty$ and $\hat{\rho} = \rho x$ finite, we get

$$y(r) = 1 + x \sum_{n=1}^{\infty} \hat{\rho}^n y_n^{(0)}(r) + \mathcal{O}(x^2) = 1 + x w(r) + \mathcal{O}(x^2), \quad (4)$$

where the second equality defines the function $w(r)$. The functions $y_n^{(0)}(r)$ are represented by *chain* diagrams, i.e.,

$$y_n^{(0)}(|\mathbf{r}_0 - \mathbf{r}_{n+1}|) = \bigcirc - \bullet - \bullet - \dots - \bullet - \bigcirc. \quad (5)$$

By application of the convolution theorem, the Fourier transform of the function $w(r)$ is given by

$$\tilde{w}(k) = \hat{\rho} [\tilde{f}_{\text{HS}}(k)]^2 [1 - \hat{\rho} \tilde{f}_{\text{HS}}(k)]^{-1}, \quad (6)$$

where $\tilde{f}_{\text{HS}}(k) = -(2\pi\sigma)^{d/2} k^{-d/2} J_{d/2}(k\sigma)$ is the Fourier transform of the HS Mayer function, $J_\nu(z)$ being the Bessel function. Similarly, the structure factor $S(k)$ and the direct correlation function $c(r)$ are

$$S(k) = [1 - \hat{\rho} \tilde{f}_{\text{HS}}(k)]^{-1} + \mathcal{O}(x), \quad (7)$$

$$c(r) = x f_{\text{HS}}(r) + \mathcal{O}(x^2). \quad (8)$$

From Eqs. (4) and (8) it follows that the PY and HNC closures become exact to first order in x . The same happens with any sensible approximation which retains the chain diagrams of the virial expansion. It is worth noting that the non-linear Debye–Hückel approximation for the radial distribution function of a system of charged particles can be derived by neglecting all but the chain diagrams, which are the most weakly connected (and hence the most strongly divergent) ones [1]. More in general, the chain diagrams determine the asymptotic long-distance behavior of the correlation functions [2].

Besides the standard structure functions of the theory of liquids listed above we have found it useful in this case to introduce an auxiliary function $\gamma(r)$ as the density integral of $w(r)$, namely $w(r) = \partial\gamma(r)/\partial\hat{\eta}$, where $\hat{\eta} = \hat{\rho} v_d \sigma^d$ is the *scaled* packing fraction, $v_d = (\pi/4)^{d/2} / \Gamma(1 + d/2)$ being the volume of a d -dimensional sphere of unit diameter. In Fourier

Table 1

Contributions of zeroth- and first-order in x to the main thermodynamic quantities

Quantity	$\mathcal{O}(x^0)$	$\mathcal{O}(x)$
$a_{\text{ex}}/k_B T$	$2^{d-1} \hat{\eta}$	$2^{d-1} \gamma(\sigma)$
$p/\rho k_B T$	$1 + 2^{d-1} \hat{\eta}$	$2^{d-1} \hat{\eta} w(\sigma)$
s_{ex}/k_B	0	$2^{d-1} \hat{\eta} [w(\sigma) - \frac{1}{2}]$
$\mu_{\text{ex}}/k_B T$	$2^d \hat{\eta}$	$2^{d-1} [\hat{\eta} - 2^{-d} w(0)]$
$u_{\text{ex}}/k_B T$	$2^{d-1} \hat{\eta}$	$2^{d-2} [\hat{\eta} - 2^{1-d} w(0)]$
c_{ex}/k_B	0	$\frac{1}{2} \hat{\eta} \partial w(0) / \partial \hat{\eta}$
$(\partial p / \partial \rho)_T / k_B T$	$1 + 2^d \hat{\eta}$	$2^{d-1} \partial [\hat{\eta}^2 w(\sigma)] / \partial \hat{\eta}$

space,

$$\tilde{\gamma}(k) = -\hat{\eta} \tilde{f}_{\text{HS}}(k) - v_d \sigma^d \ln[1 - \hat{\rho} \tilde{f}_{\text{HS}}(k)]. \quad (9)$$

We have verified that the values of $\gamma(r)$ at $r = 0$ and $r = \sigma$ satisfy the linear relation

$$\gamma(\sigma) + \frac{2^{-d}}{\hat{\eta}} \gamma(0) = \frac{\hat{\eta}}{2}, \quad (10)$$

which is crucial to prove the thermodynamic consistency between the virial and energy routes to the equation of state. By standard application of statistical-mechanical formulas relating the correlation functions to the thermodynamic quantities [1], we have derived expressions for the latter to first order in x in terms of the values of $w(r)$ and $\gamma(r)$ at $r = 0$ and $r = \sigma$. The (excess) free energy per particle a_{ex} , the compressibility factor $p/\rho k_B T$, the (excess) entropy per particle s_{ex} , the (excess) chemical potential μ_{ex} , the (excess) internal energy per particle u_{ex} , the (excess) specific heat c_{ex} and the inverse isothermal compressibility $(\partial p / \partial \rho)_T / k_B T$ are listed in Table 1. The second and third columns give the zeroth- and first-order contributions, respectively, in the exact expansions of those quantities in powers of x at constant $\hat{\rho} = \rho x$. The zeroth-order terms are linear functions of $\hat{\rho}$ (or $\hat{\eta}$), i.e., the virial expansion truncated after the second virial coefficient becomes exact in the limit $x \rightarrow 0$. However, the first-order terms are highly nonlinear functions of the scaled density and so all the virial coefficients contribute.

Gates [16] and Grewe and Klein [17] considered a class of Kac potentials of the form $\phi(r) = \epsilon \phi^*(r/\sigma)$, where $\phi^*(r^*)$ is a non-negative bounded and integrable function and $\epsilon \propto \sigma^{-d}$. They proved rigorously that in the van der Waals limit $\sigma \rightarrow \infty$, the direct

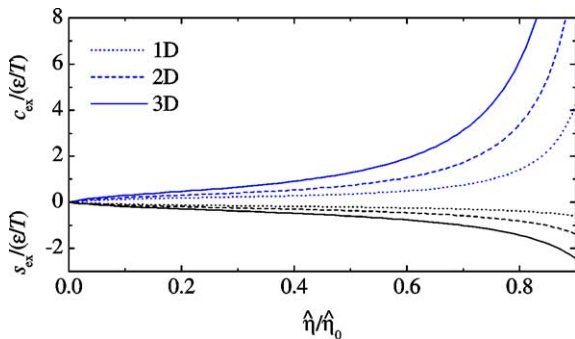


Fig. 1. Plot of $s_{\text{ex}}/(\epsilon/T)$ (lower curves) and $c_{\text{ex}}/(\epsilon/T)$ (upper curves) versus $\hat{\eta}/\hat{\eta}_0$ for $d = 1$ (dotted lines), $d = 2$ (dashed lines) and $d = 3$ (solid lines).

correlation function adopts the mean-field expression $c(r) = -\phi(r)/k_B T$ and hence the structure factor is $S(k) = [1 + (\rho/k_B T)\tilde{\phi}(k)]^{-1}$. The PS potential belongs to the Kac class with $\phi^*(r^*) = \Theta(1 - r^*)$ and so in the van der Waals limit one has $x \rightarrow 0$ with $\hat{\eta}$ fixed. It is then obvious that the van der Waals limit ($\epsilon \propto \sigma^{-d}$, $\sigma \rightarrow \infty$ at fixed T and ρ) is equivalent to the high-temperature, high-density limit (at fixed ϵ and σ) considered in this Letter. In fact, Eqs. (7) and (8) are recovered from the more general results of Refs. [16,17], although the route followed here differs from theirs. Eqs. (7) and (8) were also found by Likos et al. [5] as a mean-field approximation in the limit $\rho \rightarrow \infty$. However, as is apparent from our derivation of Eqs. (7) and (8), the key ingredient is the high-temperature assumption. The additional high-density assumption is only needed to depart from the trivial results corresponding to a gas of non-interacting particles. Comparison with Monte Carlo simulations shows that the mean-field structural functions behave very well even for $x \lesssim 0.2$ [5].

The results for the pressure, the internal energy and the isothermal compressibility to zeroth-order in x were already given by Grewe and Klein [17]. However, Eq. (10) and the third column of Table 1 are, to the best of our knowledge, new results. The contributions of $\mathcal{O}(x)$ are especially relevant in the case of the excess entropy and specific heat, since the corresponding $\mathcal{O}(x^0)$ -terms vanish. Fig. 1 shows the high-temperature limit of $s_{\text{ex}}/(\epsilon/T)$ and $c_{\text{ex}}/(\epsilon/T)$ versus $\hat{\eta}/\hat{\eta}_0$ (where $\hat{\eta}_0$ will be defined below). The non-linear density-dependence of both quantities is clearly observed.

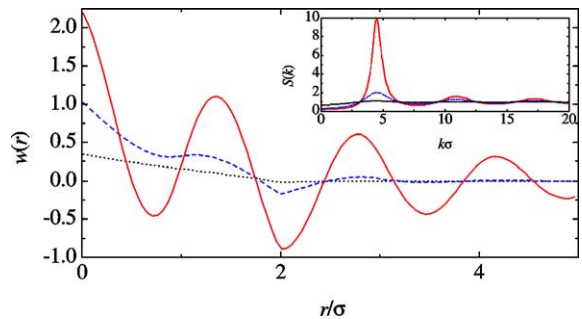


Fig. 2. Plot of $w(r)$ and $S(k)$ (see inset) at $\hat{\eta}/\hat{\eta}_0 = 0.1$ (dotted lines), 0.5 (dashed lines) and 0.9 (solid lines) for $d = 1$.

As analyzed by Grewe and Klein [17,18], the PS fluid presents a spinodal point (Kirkwood instability) at a certain scaled density. A simple examination of Eqs. (6), (7) and (9) shows that these quantities are well defined for every real wavenumber k if and only if the maximum value of $\tilde{f}_{\text{HS}}(k)$ is smaller than $1/\hat{\rho}$. In general, the absolute maximum \tilde{f}_{max} of $\tilde{f}_{\text{HS}}(k)$ occurs at k_0 , where $k_0\sigma$ is the first zero of $J_{d/2+1}(z)$. Therefore, there exists an upper bound $\hat{\rho}_0 = 1/\tilde{f}_{\text{max}}$ to the scaled density, such that the structure factor becomes divergent at the wavenumber $k = k_0$ when $\hat{\rho} \rightarrow \hat{\rho}_0$. The values of k_0 and $\hat{\eta}_0 = \hat{\rho}_0 v_d \sigma^d$ for $d = 1-5$ are displayed in the third and fifth columns of Table 2, respectively. As an illustration, in Fig. 2 we have plotted the functions $w(r)$ and $S(k)$ corresponding to the one-dimensional PS fluid for $\hat{\eta} = 0.1\hat{\eta}_0$, $0.5\hat{\eta}_0$ and $0.9\hat{\eta}_0$.

How do the structural and thermodynamic functions behave as the scaled packing fraction $\hat{\eta}$ approaches its upper bound $\hat{\eta}_0$ from below? Let us denote by $k = \pm\kappa(\hat{\eta}) \pm iq(\hat{\eta})$ (with the convention $\kappa, q > 0$) the four zeroes of $1 - \hat{\rho}\tilde{f}_{\text{HS}}(k)$ closest to the real axis in the complex k -plane. These values are responsible for the asymptotic behavior of $w(r)$ [and hence of $g(r)$] for long distances: κ is the wavenumber of the oscillations, while q is the damping coefficient, i.e., $\xi = q^{-1}$ is the *correlation length*. A straightforward asymptotic analysis yields $\kappa\sigma \approx k_0\sigma - [(d+1)/3k_0\sigma](1 - \hat{\eta}/\hat{\eta}_0)$ and

$$\xi/\sigma = (q\sigma)^{-1} \approx 2^{-1/2}(1 - \hat{\eta}/\hat{\eta}_0)^{-1/2}, \quad (11)$$

which implies that the correlation length diverges with a critical exponent $\nu = 1/2$ as the density approaches the maximum density [19]. Moreover, the correlation

Table 2

Values of the HS close-packing fraction η_{cp} , the wavenumber k_0 , the nearest-neighbor distance r_0 , the (scaled) spinodal instability packing fraction $\hat{\eta}_0$, the (scaled) freezing packing fraction $\hat{\eta}_f$, the (scaled) packing fraction $\hat{\eta}_{ms}$ at the condition of marginal stability and the (scaled) melting packing fraction $\hat{\eta}_m$

d	η_{cp}	$k_0\sigma$	r_0/σ	$\hat{\eta}_0$	$\hat{\eta}_f$	$\hat{\eta}_{ms}$	$\hat{\eta}_m$
1	1	4.49	1.40	2.30	1.00	1.00	1.00
2	$\sqrt{3}\pi/6 \simeq 0.91$	5.14	1.37	1.89	0.89	0.95	1.03
3	$\sqrt{2}\pi/6 \simeq 0.74$	5.76	1.34	1.45	0.62	0.69	0.80
4	$\pi^2/16 \simeq 0.62$	6.38	1.32	1.07	0.36	0.41	0.50
5	$\sqrt{2}\pi^2/30 \simeq 0.47$	6.99	1.30	0.76	0.22	0.26	0.33

function $w(r)$ behaves as $w(r) \approx (1 - \hat{\eta}/\hat{\eta}_0)^{-1/2}\omega(r)$, where the scaling function $\omega(r)$ is given by

$$\omega(r) = \frac{(2\pi)^{-d/2-1}}{\sqrt{2}\hat{\rho}_0\sigma^d} (k_0\sigma)^{d-1} (k_0r)^{-d/2+1} J_{d/2-1}(k_0r). \quad (12)$$

So, the first-order contribution $w(r)$ to the cavity and radial distribution functions *diverges* as $\hat{\eta}$ tends to the maximum value $\hat{\eta}_0$. On the other hand, the auxiliary function $\gamma(r)$ remains finite in that limit. According to Table 1, the first-order coefficients in x of the pressure, the entropy, the chemical potential and the internal energy diverge as $(1 - \hat{\eta}/\hat{\eta}_0)^{-1/2}$ when $\hat{\eta} \rightarrow \hat{\eta}_0$, while the coefficients of the specific heat and the isothermal compressibility diverge as $(1 - \hat{\eta}/\hat{\eta}_0)^{-3/2}$. Eq. (12) implies that $\omega(r) \sim (k_0r)^{-(d-1)/2} \cos[k_0r - (d-1)\pi/4]$ for large k_0r , so the correlations at $\hat{\eta} = \hat{\eta}_0$ oscillate with a wavenumber k_0 , the amplitude decaying algebraically. The first maximum of $\omega(r)$ (apart from the one at $r = 0$) occurs at a value $r = r_0$ such that k_0r_0 is the second zero of $J_{d/2}(z)$. The quantity r_0 represents the distance between nearest neighbors at $\hat{\eta} = \hat{\eta}_0$. It is given in Table 2 for $d = 1-5$.

On physical grounds, it is expected that the freezing transition from the stable fluid to the stable solid occurs at a scaled density $\hat{\eta}_f$ smaller than the value $\hat{\eta}_0$ at the spinodal instability. We have estimated the values of the scaled packing fraction at freezing ($\hat{\eta}_f$), at melting ($\hat{\eta}_m$) and at the point of marginal stability ($\hat{\eta}_{ms}$), by using for the PS solid phase a simple free-volume theory based on the one for the HS solid [8,20]. In the basic picture of the PS solid [6–8], the lattice sites are occupied by “clusters” of spheres that overlap each other. A particle inside one of these clusters performs random motions but excursions beyond the lattice distance are forbidden because of

the large energy cost associated with overlappings with particles in the neighbor clusters. In the high-temperature limit these clusters are expected to contain typically a large number of particles. We will suppose that, on average, this number scales as α/x (where α is a density-dependent parameter to be determined), so $\eta/(\alpha/x) = \hat{\eta}/\alpha$ is the packing fraction of the clusters. Consequently, the excess internal energy per particle of the PS solid is $u_{ex}^{solid}/k_B T = \alpha/2$. Under the assumption that every cluster behaves as a hard-core particle with a free volume $v_{free}(\hat{\eta}/\alpha)$, where

$$v_{free}(\eta) = \frac{2^d}{\rho} \left[1 - \left(\frac{\eta}{\eta_{cp}} \right)^{1/d} \right]^d \quad (13)$$

is an estimate of the free volume of a hard sphere in a crystal with packing fraction η [8,20] and η_{cp} is the HS close-packing fraction, we have estimated the excess entropy per particle of the PS solid as

$$\frac{s_{ex}^{solid}}{k_B T} = -d \ln \left[1 - \left(\frac{\hat{\eta}}{\alpha \eta_{cp}} \right)^{1/d} \right] - d \ln 2. \quad (14)$$

Given a value of $\hat{\eta}$, the parameter α is determined by minimizing the free energy $a_{ex}^{solid} = u_{ex}^{solid} + T s_{ex}^{solid}$. In this way we find that $\alpha(\hat{\eta})$ is the solution of the algebraic equation $\hat{\eta}/\eta_{cp} = \alpha^{d+1}/(2 + \alpha)^d$, so that

$$\frac{a_{ex}^{solid}(\hat{\eta})}{k_B T} = \frac{\alpha(\hat{\eta})}{2} + d \ln \left[\frac{1}{2} + \frac{\alpha(\hat{\eta})}{4} \right]. \quad (15)$$

The pressure and the excess chemical potential of the high-temperature PS solid are then $p^{solid}/\rho k_B T = 1 + \alpha(\hat{\eta})/2$, $\mu_{ex}^{solid}(\hat{\eta})/k_B T = \alpha(\hat{\eta}) + d \ln[1/2 + \alpha(\hat{\eta})/4]$. In Fig. 3 we have plotted the excess free energy per particle of the solid and the fluid phases for $d = 3$. The excess internal energy and the excess entropy of the solid are also plotted. For the fluid we

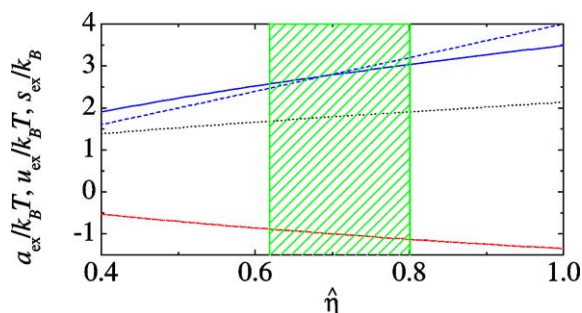


Fig. 3. Excess free energy per particle in the three-dimensional PS solid, $a_{\text{ex}}^{\text{solid}}/k_B T$ (solid line), and PS fluid, $a_{\text{ex}}^{\text{fluid}}/k_B T$ (dashed line), in the high-temperature limit. The excess internal energy, $u_{\text{ex}}^{\text{solid}}/k_B T$ (dotted line), and the excess entropy, $s_{\text{ex}}^{\text{solid}}/k_B T$ (dashed-dotted line), of the PS solid are also plotted. The shaded area represents the fluid-solid coexistence region.

have used the zeroth-order approximation given in Table 1, so $a_{\text{ex}}^{\text{fluid}}(\hat{\eta})/k_B T \approx u_{\text{ex}}^{\text{fluid}}(\hat{\eta})/k_B T \approx 2^{d-1} \hat{\eta}$ and $s_{\text{ex}}^{\text{fluid}}(\hat{\eta})/k_B \approx 0$. While the solid has a smaller entropy than the fluid, it requires less internal energy. As the density increases, the latter effect dominates over the former and the solid becomes more stable than the fluid. The (scaled) density of *marginal* stability $\hat{\eta}_{\text{ms}}$ is determined by the condition $a_{\text{ex}}^{\text{solid}} = a_{\text{ex}}^{\text{fluid}}$. The (scaled) freezing and melting densities are obtained from the equality of the pressure and the chemical potential in both phases: $p^{\text{fluid}}(\hat{\eta}_f) = p^{\text{solid}}(\hat{\eta}_m)$, $\mu_{\text{ex}}^{\text{fluid}}(\hat{\eta}_f) = \mu_{\text{ex}}^{\text{solid}}(\hat{\eta}_m)$. The values of $\hat{\eta}_m$, $\hat{\eta}_{\text{ms}}$ and $\hat{\eta}_f$ are given in Table 2 for $d = 1-5$. We observe that our heuristic estimates for the characteristic densities of the fluid–solid transition are typically less than half the upper bound density $\hat{\eta}_0$.

The one-dimensional (1D) case deserves some special comments. For $d = 1$, the curves representing the free energies of the solid and the fluid do not cross, but “kiss” each other at $\hat{\eta} = 1$ (i.e., they have the same value and slope at $\hat{\eta} = 1$). In fact, $a_{\text{ex}}^{\text{solid}}(\hat{\eta}) < a_{\text{ex}}^{\text{fluid}}(\hat{\eta})$ not only for $\hat{\eta} > 1$ but also for $\hat{\eta} < 1$. This “exaggerated” stability of the 1D PS solid for small densities is obviously an artifact of the heuristic free-volume theory we have employed. Nevertheless, our free-volume theory contains the basic ingredients explaining that the high-temperature 1D PS solid becomes more stable than the fluid at sufficiently large densities $\hat{\eta}$. This is further confirmed by the rigorous existence of the spinodal instability at $\hat{\eta}_0 \simeq 2.30$, where the metastable fluid ceases to exist and a continuous transition to a

crystalline solid takes place. We must emphasize that the fluid–solid phase transition in the 1D PS model is not forbidden by van Hove’s theorem [21] because one of the hypothesis of the theorem, requiring the interaction potential to include an infinite repulsive core that does not allow full overlaps between particles, is not fulfilled [22]. Thus, the PS model provides one of the rare examples of one-dimensional models exhibiting phase transitions [22]. Whether the fluid–solid transition occurs near $\hat{\eta} = 1$ or whether it does not present a density jump, as indicated in Table 2, are questions that need further theoretical and simulational work before being satisfactorily elucidated.

In this Letter we have focused on the high-temperature domain ($x \rightarrow 0$) of the d -dimensional PS model. When the exact diagrammatic expansion of the cavity function is considered, it turns out that x acts as an ordering parameter, so that the first-order term contains only chain diagrams, which can be easily resummed, yielding mean-field expressions. If the unscaled packing fraction η is kept finite, one arrives at the trivial case of non-interacting particles. If, on the other hand, one explores the high-density regime $\eta = \hat{\eta}/x$, much more interesting results appear. To zeroth-order in x [17] the thermodynamic quantities are described by the second virial coefficient alone, but the first-order corrections exhibit a rich non-linear dependence on $\hat{\eta}$. The fluid presents a spinodal instability at the upper bound density $\eta_0(x) = \hat{\eta}_0/x$, but this is preempted by a first-order phase transition to the solid at the freezing density $\eta_f(x) = \hat{\eta}_f/x$. It seems natural to expect that a similar situation applies for finite and low temperatures, except that the x -dependence of $\eta_0(x)$ and $\eta_f(x)$ is more complicated than in the high-temperature limit. From that point of view, it can be conjectured that the zero-temperature limit (where the PS model reduces to the HS model) of the upper bound density is $\lim_{x \rightarrow 1} \eta_0(x) = \eta_{\text{cp}}$. Analogously, $\lim_{x \rightarrow 1} \eta_f(x) = \eta_f^{\text{HS}}$, where η_f^{HS} is the freezing packing fraction of the HS fluid. Since $\eta_{\text{cp}} < \hat{\eta}_0$ (cf. Table 2) and $\eta_f^{\text{HS}} < \hat{\eta}_f$, it seems plausible that the products $x\eta_0(x)$ and $x\eta_f(x)$ are smoothly decreasing functions of x bounded between the values $\hat{\eta}_0$ and $\hat{\eta}_f$, respectively, at $x = 0$ and the values η_{cp} and η_f^{HS} , respectively, at $x = 1$. This suggests the possibility of constructing a simple approximate theory for the PS model spanning the whole temperature spectrum, by interpolating between the successful PY theory for

hard spheres (zero temperature) and the mean-field-theory results (high temperatures). We are currently working along these lines and further results will be published elsewhere.

Acknowledgements

We are grateful to J.A. Cuesta, J.W. Dufty, E. Lomba, A. Malijevský, A. Sánchez and M. Silbert for useful discussions about the topic of this Letter. This work has been partially supported by the Ministerio de Ciencia y Tecnología (Spain) through grant No. BFM2001-0718 and by the European Community's Human Potential Programme under contract HPRN-CT-2002-00307, DYGLAGEMEM.

References

- [1] J.-P. Hansen, I.R. McDonald, *Theory of Simple Liquids*, Academic Press, London, 1986.
- [2] G.A. Martynov, *Fundamental Theory of Liquids. Method of Distribution Functions*, Hilger, Bristol, 1992.
- [3] E. Thiele, *J. Chem. Phys.* 39 (1963) 474;
M.S. Wertheim, *Phys. Rev. Lett.* 10 (1964) 321;
R.J. Baxter, *J. Chem. Phys.* 49 (1968) 2770.
- [4] F.H. Stillinger, D.K. Stillinger, *Physica A* 244 (1997) 358;
H. Graf, H. Löwen, *Phys. Rev. E* 57 (1998) 5744;
A. Lang, C.N. Likos, M. Watzlawek, H. Löwen, *J. Phys.: Condens. Matter* 12 (2000) 5087;
A.A. Louis, P.G. Bolhuis, J.-P. Hansen, *Phys. Rev. E* 62 (2000) 7961;
- R. Finken, J.-P. Hansen, A.A. Louis, *J. Stat. Phys.* 110 (2003) 1015.
- [5] C.N. Likos, A. Lang, M. Watzlawek, H. Löwen, *Phys. Rev. E* 63 (2001) 031206.
- [6] C.N. Likos, *Phys. Rep.* 348 (2001) 267, and references therein.
- [7] W. Klein, H. Gould, R.A. Ramos, I. Clejan, A.I. Mel'cuk, *Physica A* 205 (1994) 738.
- [8] C.N. Likos, M. Watzlawek, H. Löwen, *Phys. Rev. E* 58 (1998) 3135.
- [9] M. Schmidt, *J. Phys.: Condens. Matter* 11 (1999) 10163.
- [10] M.J. Feraud, E. Lomba, L.L. Lee, *J. Chem. Phys.* 112 (2000) 810;
N. Choudhury, S.K. Ghosh, *J. Chem. Phys.* 119 (2003) 4827.
- [11] Y. Rosenfeld, M. Schmidt, M. Watzlawek, H. Löwen, *Phys. Rev. E* 62 (2000) 5006.
- [12] M. Schmidt, M. Fuchs, *J. Chem. Phys.* 117 (2002) 6308.
- [13] S.-C. Kim, S.-Y. Suh, *J. Chem. Phys.* 117 (2002) 9880.
- [14] C.N. Likos, H. Löwen, M. Watzlawek, B. Abbas, O. Jucknischke, J. Allgaier, D. Richter, *Phys. Rev. Lett.* 80 (1998) 4450;
M. Watzlawek, C.N. Likos, H. Löwen, *Phys. Rev. Lett.* 82 (1999) 5289.
- [15] C. Marquest, T.A. Witten, *J. Phys. (France)* 50 (1989) 1267.
- [16] D.J. Gates, *Physica A* 81 (1975) 47.
- [17] N. Grewe, W. Klein, *J. Math. Phys.* 18 (1977) 1729, 1735.
- [18] W. Klein, N. Grewe, *J. Chem. Phys.* 72 (1980) 5456.
- [19] W. Klein, A.C. Brown, *J. Chem. Phys.* 78 (1981) 6960.
- [20] E. Velasco, L. Mederos, G. Navascués, *Mol. Phys.* 97 (1999) 1273;
R. Finken, M. Schmidt, H. Löwen, *Phys. Rev. E* 65 (2002) 0161008.
- [21] L. van Hove, *Physica A* 16 (1950) 137;
D. Ruelle, *Statistical Mechanics: Rigorous Results*, Addison-Wesley, Reading, MA, 1989.
- [22] J.A. Cuesta, A. Sánchez, *J. Phys. A: Math. Gen.* 35 (2002) 2373;
J.A. Cuesta, A. Sánchez, *J. Stat. Phys.* (2004), in press.